Original Article
Upregulation of circRNA_0023685 promotes gastric cancer progression via a circRNA-miRNA-mRNA interaction network

You-Ci Zhou[1*], Wen-Ji Lao[1*], Yi-Lu Xu[2], Xi Huang[3], Chen Li[4], Zhen-Qiang Wang[4], Qi-Jun Wang[5*], Yun-Wei Sun[1*]

[1]Department of Gastroenterology, Ruijin Hospital, Shanghai Jiao Tong University School of Medicine, Shanghai, China; [2]Hongqiao International Institute of Medicine, Shanghai Tongren Hospital, Key Laboratory of Cell Differentiation and Apoptosis of Chinese Ministry of Education, Faculty of Basic Medicine, Shanghai Jiao Tong University School of Medicine, Shanghai, China; [3]Department of Intensive Care Medicine, Renji Hospital Affiliated to Shanghai Jiao Tong University School of Medicine, Shanghai, China; [4]Department of General Surgery, Shanghai Key Laboratory of Gastric Neoplasms, Shanghai Institute of Digestive Surgery, Ruijin Hospital, Shanghai Jiao Tong University School of Medicine, Shanghai, China; [5]Faculty of Medical Laboratory Science, Ruijin Hospital, Shanghai Jiao Tong University School of Medicine, Shanghai, China. *Equal contributors.

Abstract: Circular RNAs (circRNAs) have been extensively studied for their critical roles as noncoding RNAs (ncRNAs) in gastric cancer (GC). In this study, we focused on the expression, function and molecular mechanism of circRNA_0023685 in gastric cancer (GC) to provide new ways for the diagnosis and treatment of GC. Firstly, a novel differentially expressed circRNA, circRNA_0023685, was identified, and its differential expression in GC plasma, tissue, and cell lines was further verified by RT-qPCR. Next, circRNA_0023685 was verified to promote the proliferation, migration and apoptosis of GC cells in vitro. CircRNA_0023685 was also proved to enhance the growth of GC tumors in xenograft models. Finally, for excavating the mechanism to promote GC, downstream microRNAs (miRNAs) and mRNAs were screened by bioinformatics analyses. After intersecting the target genes and genes enriched in GO analysis, a circRNA competing endogenous RNAs (ceRNAs) network was built. A protein-protein interaction (PPI) network was then constructed to find the candidate gene, APP. Our study confirmed that the highly expressed circRNA_0023685 could promote GC, which provided a new clinical diagnostic biomarker and therapeutic target for GC.

Keywords: Circular RNA, gastric cancer, circRNA-miRNA-mRNA, bioinformatics

Introduction

Gastric cancer (GC) is the fifth most common cancer overall and the fourth most common cause of cancer-related mortality worldwide, according to epidemiological data [1, 2]. Carcinoembryonic antigen (CEA), carbohydrate antigen (CA), pepsinogen (PG) and alpha-fetoprotein (AFP) are the most commonly used clinical tumor markers for the early diagnosis of GC [3]. However, the specificity and sensitivity of these serum indicators are subpar, and none are currently specific for the diagnosis of GC [3-5]. Therefore, it is essential to identify new tumor markers for early detection of GC and examine their likely underlying mechanisms.

Due to their increased stability compared to other RNAs, circular RNAs (circRNAs) have recently demonstrated promise as biomarkers for the modeling of human cancer [6, 7]. It is generally accepted that the vast majority of circRNAs are exonic circRNAs (ecircRNAs), which are primarily the products of back-splicing events; during these events, exons are spliced in such a way that an upstream exon can be joined to a downstream exon, resulting in covalently closed circRNA molecules, which are more likely than linear mRNAs to maintain a stable structure with lower susceptibility to degradation by RNase R [8, 9]. Accumulating studies have shown that circRNAs can be used as a new type of tumor marker for cancers such as

GC, lung adenocarcinoma and breast cancer because they can be detected in liquid biopsy samples such as plasma, saliva and urine samples [10-13]. CircRNAs have also been reported to regulate GC development and progression [14]. CircRNAs have been demonstrated to act as microRNA (miRNA) sponges, regulate selective splicing, bind to RNA-binding proteins (RBPs), and encode proteins. Sponging of miRNAs is the best-described mode of action for circRNAs based on high-throughput RNA sequencing and bioinformatic analyses [15].

Importantly, hsa_circ_0023685 was discovered in our study by combined microarray analysis of circRNAs in plasma samples from GC patients and bioinformatic analysis of the Gene Expression Omnibus (GEO) dataset GSE-93541. CircRNA_0023685 showed increased expression in plasma and tissues of GC patients compared to those of healthy controls, indicating its potential as a biomarker for GC. The participation of circRNA_0023685 in the development of GC was then demonstrated both *in vitro* and *in vivo*. Additionally, using biosignature analysis, the biological activities and potential molecular pathways of circRNA_0023685 were investigated. The MiRanda, TargetScan, starBase, and GEO databases were used to screen for downstream miRNAs, which were then subjected to weighted gene coexpression network analysis (WGCNA) and Gene Ontology (GO) enrichment analysis. The predominant mechanism of GC formation induced by circRNA_0023685 was about cell division. CircRNA_0023685 regulated the expression of amyloid beta precursor protein (APP) as a prognostic target via miRNA sponging. To identify new targets for the clinical diagnosis and therapy of GC, we aimed to reveal the functional, prognostic and predictive roles of circRNA_0023685 in GC.

Material and methods

Microarray data analysis

Sample preparation and microarray hybridization were performed based on Arraystar's standard protocols. Agilent Feature Extraction software (version 11.0.1.1) was used to analyze the acquired array images. Quantile normalization and subsequent data processing were performed using the *limma* package in R software. CircRNAs with significant differential expression between the two groups were identified through volcano plot filtering. Differentially expressed circRNAs (DECs) between two samples were identified through fold change filtering. Hierarchical clustering was performed to visualize the distinguishable circRNA expression patterns among the samples.

The raw GSE93541 data were downloaded from the GEO database and analyzed using R software. The *limma* package was used to screen for DECs, and circRNAs with an expression fold change of ≥ 1.5 and a false discovery rate (FDR)-adjusted *p* value of < 0.05 were considered to be significantly differentially expressed.

GC tissues and plasma

A total of 34 pairs of GC tissues and adjacent normal tissues (ANTs) were collected from Ruijin Hospital of Shanghai Jiao Tong University School of Medicine. In addition, plasma samples from 34 GC patients and 23 healthy controls were obtained to assess the diagnostic value of plasma circRNA_0023685. All study protocols were approved by the ethics committee of Ruijin Hospital of Shanghai Jiao Tong University School of Medicine.

Cell culture

The human GC cell lines MKN45, SGC7901, MGC803 and BGC823 and the normal human gastric epithelial cell line GES-1 were purchased from the American Type Culture Collection (ATCC) (Manassas, USA). MKN45, SGC7901, MGC803, BGC823 and GES-1 cells were cultured in DMEM supplemented with 10% fetal bovine serum (FBS) (HyClone, USA), 1% penicillin/streptomycin (10,000 μg/ml) (Invitrogen, USA). All cells were maintained in a 5% CO_2 humidified atmosphere at 37°C.

Virus production and infection

The lentiviral plasmid (pLKO.1-shRNA; 16 μg), as well as the packaging plasmid psPAX2 (12 μg) and the envelope plasmid pMD2.G (4 μg), were cotransfected into 293T cells using the $CaCl_2$ transfection system. Virus-containing supernatants were collected and filtered 48 h and 72 h post-transfection. A GC cell line (MKN45) was infected with the collected virus-containing supernatant by centrifugation at

Table 1. The sequences of primers

Name	Sequence (5'-3')
circRNA_0023685-F	TTCTTCTAATGCCTTGTAGC
circRNA_0023685-R	GTGCTGGTATTTCTCATCG
β-actin-F	CACCATTGGCAATGAGCGGTTC
β-actin-R	AGGTCTTTGCGGATGTCCACGT
sh-2-F	CCGGCTTCTAATGCCTTGTAGCTGCCTCGAGGCAGCTACAAGGCATTAGAAGTTTTTG
sh-2-R	AATTCAAAAACTTCTAATGCCTTGTAGCTGCCTCGAGGCAGCTACAAGGCATTAGAAG
sh-4-F	CCGGTCTAATGCCTTGTAGCTGCTGCTCGAGCAGCAGCTACAAGGCATTAGATTTTTG
sh-4-R	AATTCAAAAATCTAATGCCTTGTAGCTGCTGCTCGAGCAGCAGCTACAAGGCATTAGA

2000 rpm and 37°C for 2 h in the presence of 4 μg/ml polybrene, and the cells were then cultured for at least 2 h at 37°C in an incubator with 5% CO_2. The sequences of the shRNAs are listed in **Table 1**.

RNA extraction and reverse transcription-quantitative polymerase chain reaction (RT-qPCR)

Total RNA was extracted from patient plasma using the miRNeasy Serum/Plasma Kit (Qiagen, Germany) according to the manufacturer's instructions. RNA was reverse transcribed into cDNA using Reverse Transcriptase XL (AMV) (Takara, China). Then, 2 × Taq Master Mix (Dye Plus) (Vazyme, China) was used for PCR. For RT-qPCR analysis of circRNAs and other RNAs, ChamQ Universal SYBR qPCR Master Mix (Vazyme, China) was used. The sequences of the primers used for PCR are listed in **Table 1**. Relative expression levels of circRNAs were calculated using the $2^{-\Delta\Delta Ct}$ method, and β-actin was used as a control.

Cell counting kit-8 (CCK-8) assay

Cell viability was determined with CCK-8 (Yeasen, China) according to the manufacturer's instructions. In brief, GC cells were seeded into 96-well plates (approximately 2,000 cells per well) and cultured, and 10 μl of CCK-8 solution was added to each well 1, 3 and 5 d after seeding. The cells were incubated with the CCK-8 solution for 2 h. Next, the absorbance of the wells was measured at 450 nm with a microplate reader (BioTek, USA).

Transwell migration assay

A total of 300 μl of the cell suspension (6 × 10⁴ cells) was added to the upper chambers of a Transwell culture plate (Jetbiofil, China). To the bottom chambers, 800 μl of medium containing 10% FBS was added. The plate was incubated at 37°C and 5% CO_2 for 24 h. The cells were fixed with 4% paraformaldehyde fixative solution (Beyotime, China) for 30 min. After washing with PBS, the cells were stained with crystal violet (Beyotime, China) for 15 min. Then, the cells on the upper surface of the polycarbonate filters were gently removed with wet cotton swabs. The migration rate was finally calculated by counting the cells on the lower surface of the membrane.

Scratch assay

A scratch assay was conducted to further evaluate the cell migration capacity. Transfected cells were seeded into 6-well plates at a density of 5 × 10⁵ cells/well. When the cells were 100% confluent, the cell monolayer was scratched with a 200 μl pipette tip, and the plates were then incubated in fresh serum-free medium for 24 h at 37°C with 5% CO_2.

Apoptosis assay

After transfection, apoptosis in GC cells was quantified by an Annexin V Apoptosis Detection Kit (Beyotime, China). Cells were mixed with 5 μl of Annexin V-APC and incubated for 15 min at room temperature in the dark. The cells were then washed twice and stained with 10 μl of propidium iodide (PI). FlowJo software (BD Biosciences, USA) was used to calculate the percentage of apoptotic cells.

Xenograft models

All animal breeding and other experimental operations were performed in accordance with the relevant management requirements/guidelines and ethical requirements for animal

experiments. NOG mice (female, 8 weeks old) were obtained from Shanghai Jiao Tong University School of Medicine, housed in a specific pathogen-free (SPF)-grade facility with free access to water and food, and divided into a control group and an experimental group (10 mice per group). GC cells were transfected with short hairpin RNAs (shRNAs) and injected subcutaneously into NOG mice. The volume (V = length × width^2 × 0.5) of the xenograft tumors was measured every week. The mice were sacrificed 4 weeks after cell inoculation, and the subcutaneous tumors were harvested and weighed.

Construction of the gene co-expression network and identification of significant modules

Based on the scale-free topology criterion, the co-expression network in the datasets (GSE-116312, GSE79973, GSE56807, GSE65801 and GSE113255) was constructed by weighted gene co-expression network analysis (WGCNA). The soft threshold power value was selected using the *pickSoftThreshold* function from the R package *WGCNA*, followed by building a scale-free co-expression network. Finally, co-expression modules were identified by dynamic tree cut method with the minimum module size set to 30. Modules with high similarity scores were merged with a threshold value for each dataset.

Construction of protein-protein interaction (PPI) network

To investigate the function of GC-related mRNAs, Gene Ontology (GO) analyses were performed. FDR < 0.05 was considered as statistical significance. After intersecting the predicted mRNAs, the ceRNA network was visualized by Cytoscape software (https://cytoscape.org/). To further explore the interaction between the mRNAs in the ceRNA regulatory network, the PPI network was performed by using the STRING database. The CytoHubba plug-in was used to filter core mRNAs by intersecting the first 10 mRNAs of the degree algorithm.

Survival analysis

The APP expression levels between GC tissue and normal tissue were compared by Gene Expression Profiling Interactive Analysis (GEPIA) (http://gepia.cancer-pku.cn/). Survival analyses were conducted with the Kaplan-Meier Plotter (http://kmplot.com) database. The final prognostic KM plots were demonstrated with a hazard ratio (HR), 95% confidence interval (CI) and log-rank *p* value. A *p* value < 0.05 was considered statistically significant. Protein expression of APP in both GC and normal tissues was retrieved from the Human Protein Atlas (www.proteinatlas.org).

Statistical analysis

Quantitative data are presented as the means ± standard deviations, and all experiments were repeated more than 3 times. Comparisons between two groups and among more than two groups were performed by Student's t test and one-way analysis of variance (ANOVA), respectively. The diagnostic utility of plasma circRNA_0023685 was analyzed using receiver operating characteristic (ROC) curves. All statistical analyses were performed using SPSS software, version 26.0 and GraphPad Prism, version 8.00. Different significance threshold values were used: $P < 0.05$ (*), $P < 0.01$ (**) and $P < 0.001$ (***).

Results

Plasma circRNA expression profiles in GC patients and healthy controls

To study the potential roles of circRNAs in GC, circRNA microarray analysis was performed on nine samples of human plasma collected from six GC patients and three healthy controls. CircRNA expression profiles were evaluated by microarray hybridization. The variations in circRNA expression between the two groups were visualized by hierarchical clustering (**Figure 1A**). A scatter plot of the circRNA expression profile data was generated to characterize the variations in plasma circRNA expression between GC patients and healthy controls (**Figure 1B**). The statistical significance of differential circRNA expression between the two groups was additionally visualized using a volcano plot (**Figure 1C**). Considering that false positives can be caused by multiple comparisons, we used FDR correction to adjust the *p* values. After FDR correction, 6 DECs with fold change ≥ 1.5 and *P* < 0.05 were identified, specifically, 3 significantly upregulated and 3 significantly downregulated circRNAs. Additionally,
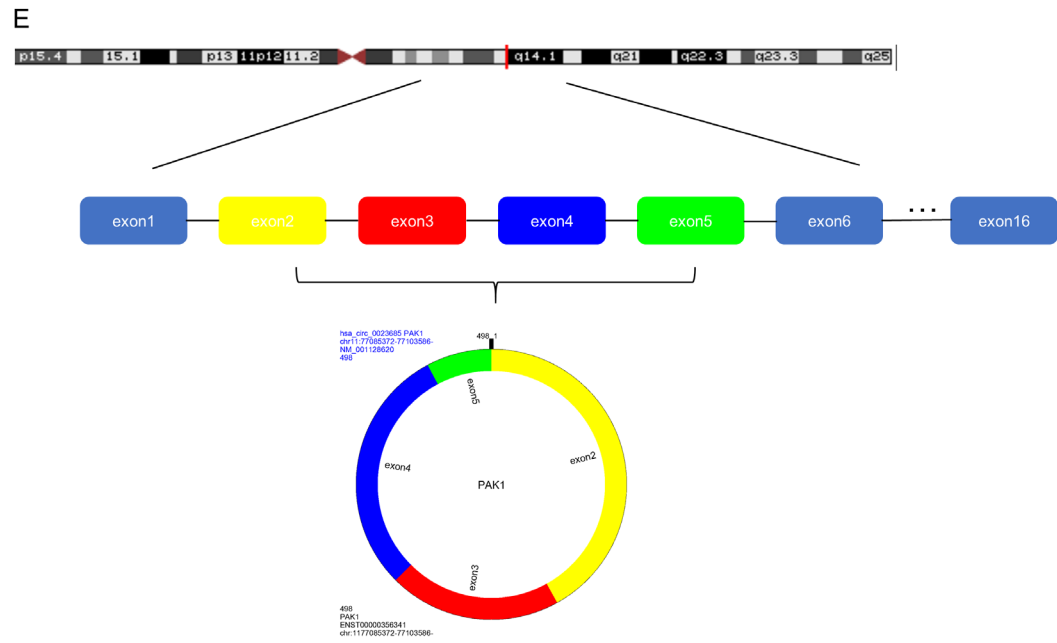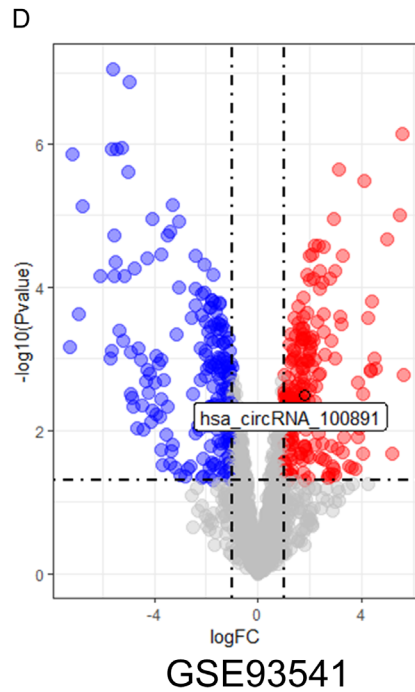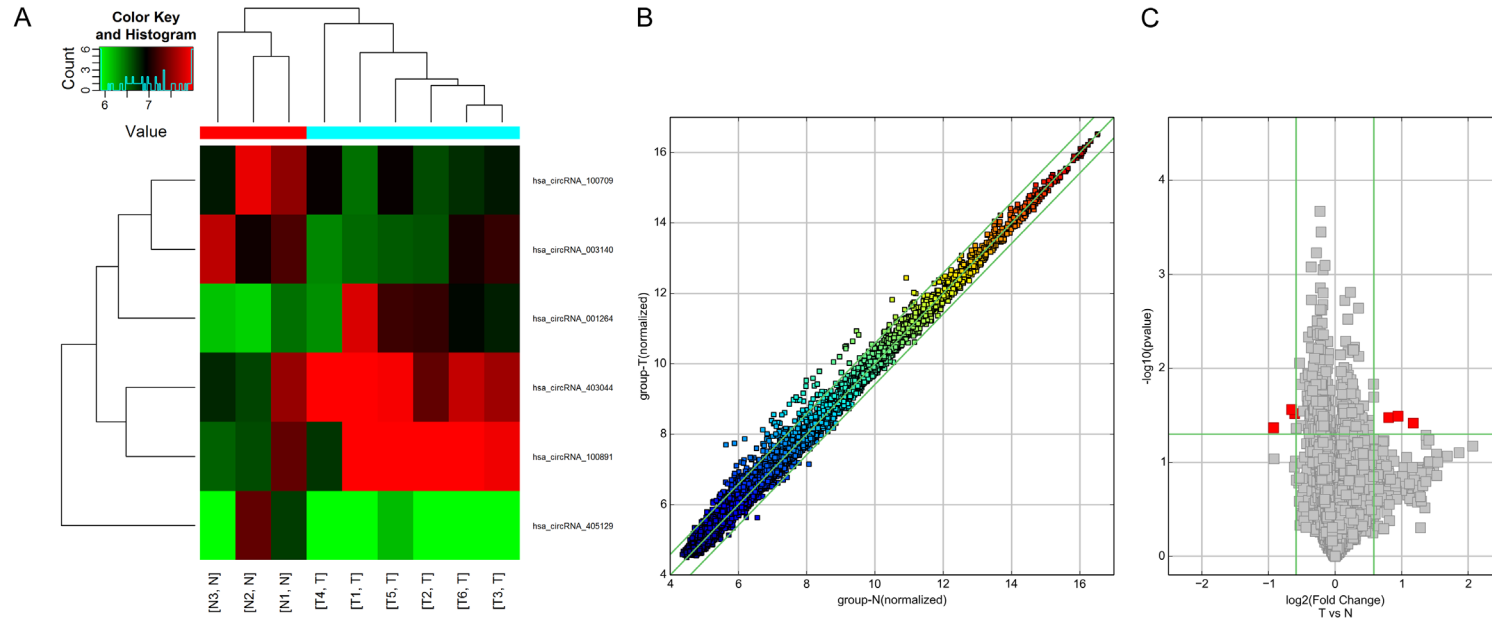
CircRNA-miRNA-mRNA interaction network affecting the GC progression

Figure 1. Overview of microarray signatures. (A) Heatmap, (B) scatter plot and (C) volcano plot of circRNA expression profiles from the microarray analysis in the two groups. (D) One overlapping differentially expressed exonic circRNAs shown in the volcano plot visualizing the DECs between the plasma samples from patients with cancer and healthy controls in GSE93541. (E) Schematic diagram of the mRNA back-splicing event that forms circRNA_0023685, which is a covalently closed loop.
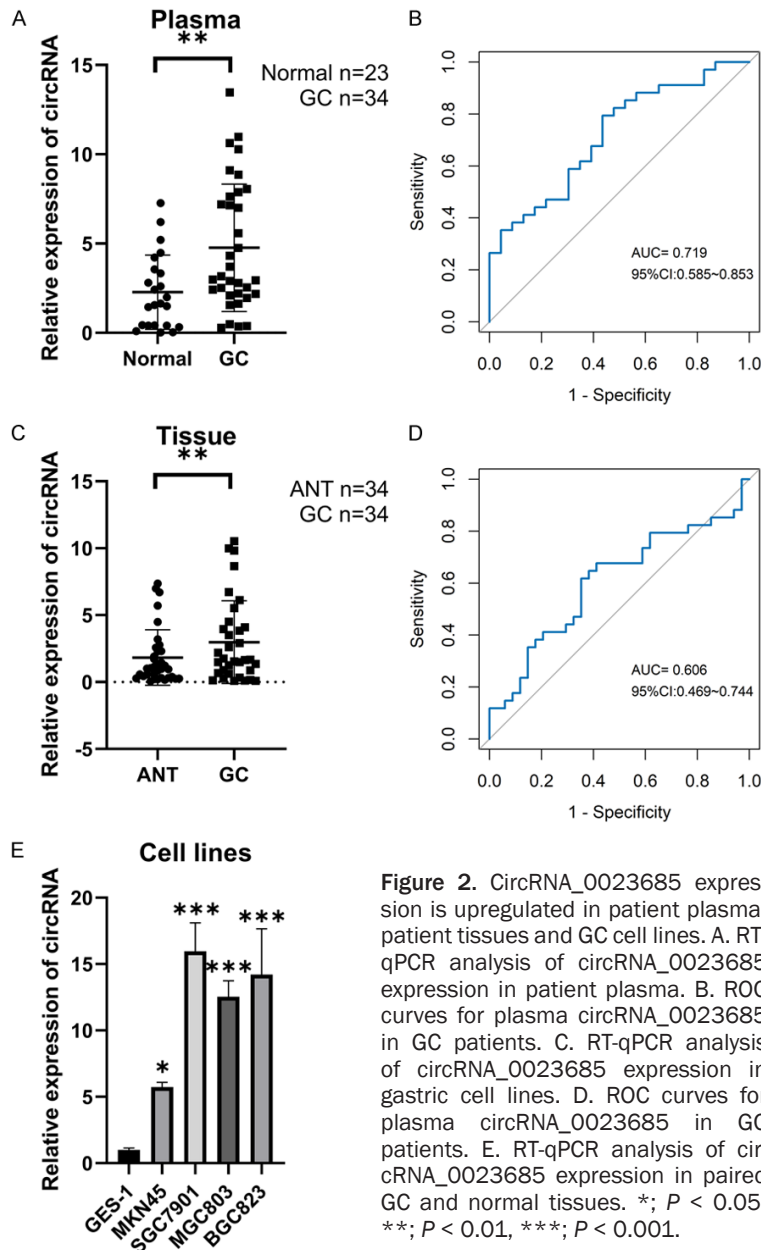
Figure 2. CircRNA_0023685 expression is upregulated in patient plasma, patient tissues and GC cell lines. A. RT-qPCR analysis of circRNA_0023685 expression in patient plasma. B. ROC curves for plasma circRNA_0023685 in GC patients. C. RT-qPCR analysis of circRNA_0023685 expression in gastric cell lines. D. ROC curves for plasma circRNA_0023685 in GC patients. E. RT-qPCR analysis of circRNA_0023685 expression in paired GC and normal tissues. *; $P < 0.05$, **; $P < 0.01$, ***; $P < 0.001$.

CircRNA_0023685 is derived from the p21 (RAC1) activated kinase 1 (PAK1) gene located at chr11:77085372-771035-86 and has a length of 214 nt. A schematic diagram showing the formation of circRNA_0023685 from PAK1 pre-mRNA (exons 2, 3, 4 and 5) is shown in **Figure 1E**.

CircRNA_0023685 was highly expressed in GC patient tissues and plasma samples and in GC cell lines

To verify the changes in the circRNA_0023685 expression level in GC patients, plasma samples were collected from 34 GC patients and 23 healthy individuals as controls. The higher plasma level of circRNA_0023685 in GC patients was corroborated by RT-qPCR ($P = 0.0039$), consistent with the sequencing results (**Figure 2A**). ROC curves were used to evaluate the diagnostic efficiency of the circRNA_0023685 level in both plasma and tissue for GC. The ROC curves of plasma circRNA_0023685 showed that it had an area under the curve (AUC) of 0.719 (95% CI: 0.585-0.853) (**Figure 2B**). In addition, to further validate the level of circRNA_0023685, we examined its level in 34 pairs of GC tissues and ANTs. The RT-qPCR results showed

the GSE93541 dataset in the GEO database, which contained expression data for plasma samples from 3 GC patients and 3 healthy controls, was analyzed. After overlapping the identified DECs, the only multiexonic circRNA was selected for further study: hsa_circ_100891, also known as hsa_circ_0023685 (**Figure 1D**).

that the circRNA_0023685 level was similarly significantly increased in GC tissues ($P = 0.0053$) (**Figure 2C**). To assess the potential diagnostic value of tissue circRNA_0023685, we performed another ROC analysis and calculated an AUC of 0.606 (95% CI: 0.469-0.744) (**Figure 2D**). Furthermore, we performed

RT-qPCR on GC cell lines and normal gastric epithelial cells and found consistent results of higher circRNA_0023685 expression in the GC cell lines ($P < 0.05$) (**Figure 2E**).

CircRNA_0023685 knockdown reduced GC cell proliferation, migration and apoptosis in vitro

Given that the microarray analysis showed that circRNA_0023685 was overexpressed in GC, we constructed a plasmid for downregulation of circRNA_0023685 to explore its potential functional role. To this end, we designed five shRNAs targeting the circular splice junction of circRNA_0023685 to knock down its expression. To verify the knockdown efficiency of the shRNAs, RT-qPCR was performed. The two shRNAs with the highest knockdown efficiency, sh-2 and sh-4 ($P < 0.001$), were selected for subsequent cell functional assays (**Figure 3A**). To investigate the biological role of the circRNA of interest, two shRNAs targeting circRNA_0023685 and a scrambled shRNA as a normal control were transfected into the GC cell line MKN45. CircRNA_0023685 downregulation decreased proliferation compared with that in the control group, according to the CCK8 assay ($P < 0.001$) (**Figure 3B**). The scratch assay and transwell migration assay showed that circRNA_0023685 silencing significantly inhibited the migration of MKN45 cells (**Figure 3C, 3D**). Moreover, flow cytometric analysis indicated that circRNA_0023685 downregulation increased the frequency of spontaneous apoptosis in MKN45 cells ($P < 0.01$) (**Figure 3E**). All the above experimental results suggest that circRNA_0023685 has an important potential role in the development of GC.

CircRNA_0023685 knockdown reduced the growth of GC tumors in vivo

To further verify that circRNA_0023685 also had an important role in the growth of GC *in vivo*, stable GC cell lines with loss of function of circRNA_0023685 were constructed. After subcutaneous injection of GC cells with low expression of circRNA_0023685, tumor growth was monitored in NOG mice, and volumetric data were recorded weekly (**Figure 4A**). Consistent with the *in vitro* cell growth assay results, mice in the circRNA knockdown groups exhibited slower tumor growth, and smaller tumors were obtained when the mice were sac-

rificed after 4 weeks of observation (**Figure 4B-D**). In addition, RT-qPCR analysis showed that circRNA_0023685 expression was decreased in the tumor tissues of mice in the circRNA depletion groups ($P < 0.001$) (**Figure 4E**). Collectively, the results of the *in vivo* and *in vitro* experiments more fully elucidated that circRNA_0023685 plays a promotive role in the pathogenesis of GC.

CircRNA_0023685 could act as a miRNA sponge to regulate gene expression in GC

CircRNA_00238685 may be involved in the development of GC by sponging miRNAs and thereby deregulating the repressive effects of miRNAs on their target genes. Therefore, miRanda, TargetScan and starBase were used to predict the miRNAs that might bind to circRNA_0023685, and the predicted binding miRNAs were overlapped with the differentially expressed miRNAs identified in GSE224056 and GSE158315. Ultimately, we obtained eight likely target miRNAs: hsa-miR-3612, hsa-miR-3064-5p, hsa-miR-542-3p, hsa-miR-4731-5p, hsa-miR-2467-3p, hsa-miR-5691, hsa-miR-338-3p and hsa-miR-185-5p (**Figure 5A**). As shown in the figure, these miRNAs contained possible binding sites for circRNAs and mRNAs (**Figure 5B, 5C**). Based on these 8 miRNAs, 430 target mRNAs were also predicted by miRanda and TargetScan (**Figure 5D**).

Enrichment analysis of the genes related to GC

To better understand the potential molecular functions of mRNAs in GC, WGCNA was conducted in the GSE116312, GSE79973, GSE56807 and GSE65801 datasets after normalization. With the settings of a scale-free $R^2 > 0.85$ and the mean connectivity of all genes < 150, a value of 6 was chosen as the best soft threshold (power) in our study (**Figure 6A**). The initialized and merged modules were finally displayed below the clustering tree (**Figure 6B**). A total of 14 coexpression modules were classified using cluster analysis, and a cluster dendrogram is shown. Three modules, "greenyellow", "darkseagreen3" and "blue2", were positively correlated with GC and were selected as GC correlation modules (**Figure 6C**). 230 mRNAs in the three modules were used to evaluate their biological roles. The top 20 GO terms of each group were demonstrated in **Figure 6D-F**. In the biological process (BP) cat-
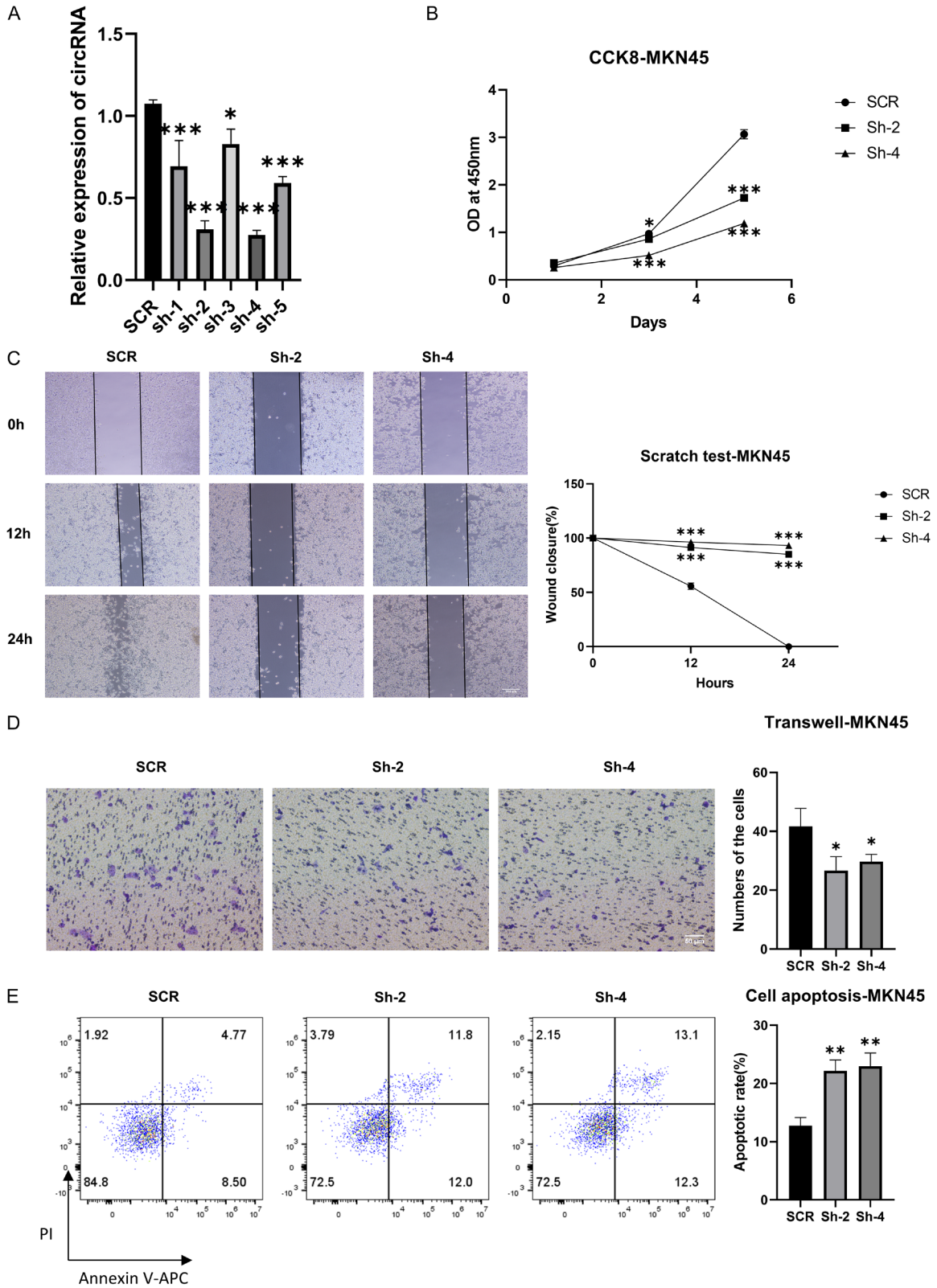
Figure 3. Effect of circRNA_0023685 downregulation on the proliferation, migration, apoptosis and other behaviors of MKN45 cells. (A) RT-qPCR analysis of the knockdown efficiency of these shRNAs. (B) A CCK8 assay was performed to assess the proliferation of MKN45 cells after transfection. (C) Scratch assay. (D) A transwell assay was performed to assess the migration of MKN45 cells after transfection. (E) Flow cytometry was used to analyze apoptosis in MKN45 cells after transfection. Bar = 200 μm (C), 50 μm (D). *; $P < 0.05$, **; $P < 0.01$, ***; $P < 0.001$.
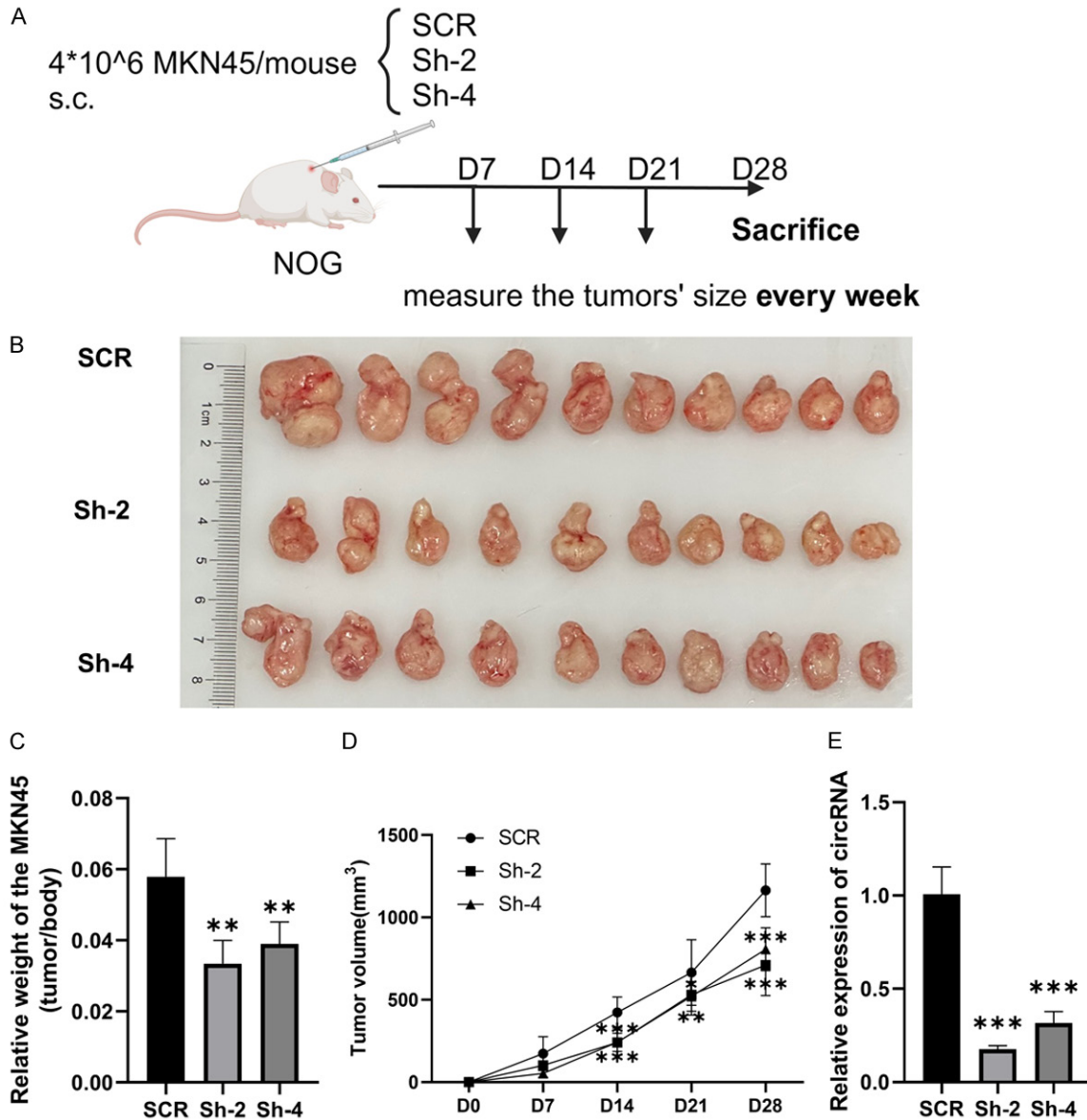
Figure 4. CircRNA_0023685 depletion inhibits tumor growth *in vivo*. (A) Schematic diagram of the mouse subcutaneous xenograft model (created with Biorender.com). (B) Tumor image, (C) tumor volume and (D) relative tumor weight in the normal control and circRNA_0023685-silenced groups. (E) RT-qPCR analysis of circRNA_0023685 expression in subcutaneous tumor tissues. **; $P < 0.01$, ***; $P < 0.001$.

egory, the main enriched categories were nuclear division, organelle fission, mitotic nuclear division, chromosome segregation and mitotic cell cycle phase transition (**Figure 6D**). In the molecular function (MF) category, extracellular matrix structural constituent, platelet-derived growth factor binding and collagen binding were enriched (**Figure 6E**). In the cellular component (CC) category, collagen-containing extracellular matrix, chromosomal region and condensed chromosome were significantly enriched in the positively correlated genes (**Figure 6F**). Based on GO enrichment analysis of the datasets, the process about cell division is highly related to GC. Additionally, immune-related pathways were also founded in GSE113255, which provided another explanation for the mechanism of circRNA_0023685 promoting GC (Supplementary Figure 1).
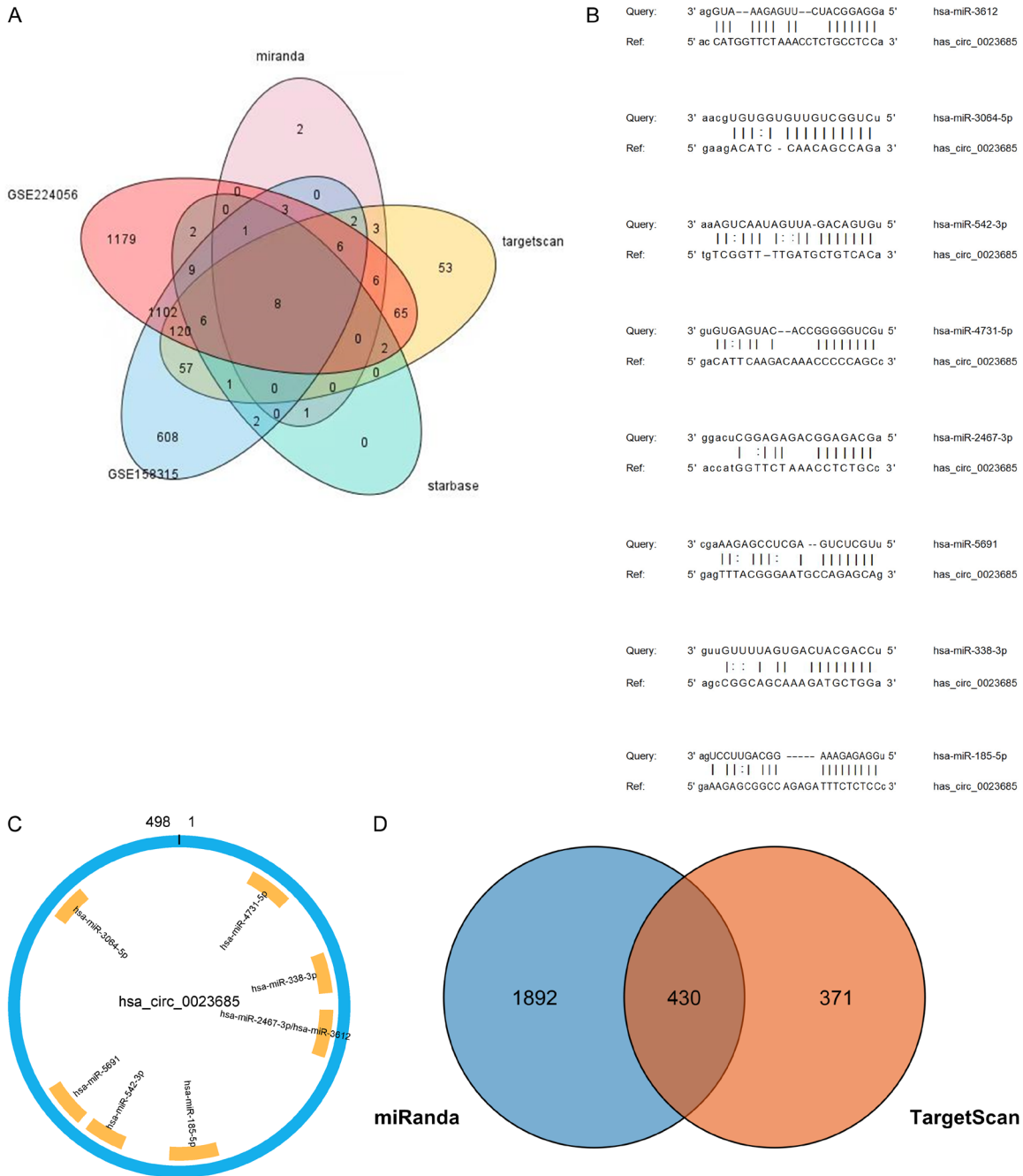
Figure 5. Prediction of miRNAs and mRNAs targeted by circRNA_0023685. A. Eight target miRNAs were predicted by the miRanda, TargetScan, starBase and GEO databases. B, C. Possible binding sites for circRNAs and miRNAs. D. 430 target mRNAs were predicted by miRanda and TargetScan.

APP as a prognostic target to promote GC via a circRNA-miRNA-mRNA network

Considering the function of circRNA_0023685 on cell proliferation, migration and apoptosis, genes in the process about cell division were chosen. There were 26 shared genes between

the 868 genes in the top 5 most enriched significantly BPs and the 430 predicted genes (**Figure 7A**). The circRNA-miRNA-mRNA network was constructed with 1 circRNA, 8 miRNAs and 26 mRNAs (**Figure 7B**). According to STRING database, a PPI network was established to show the interactions of the 26 target genes
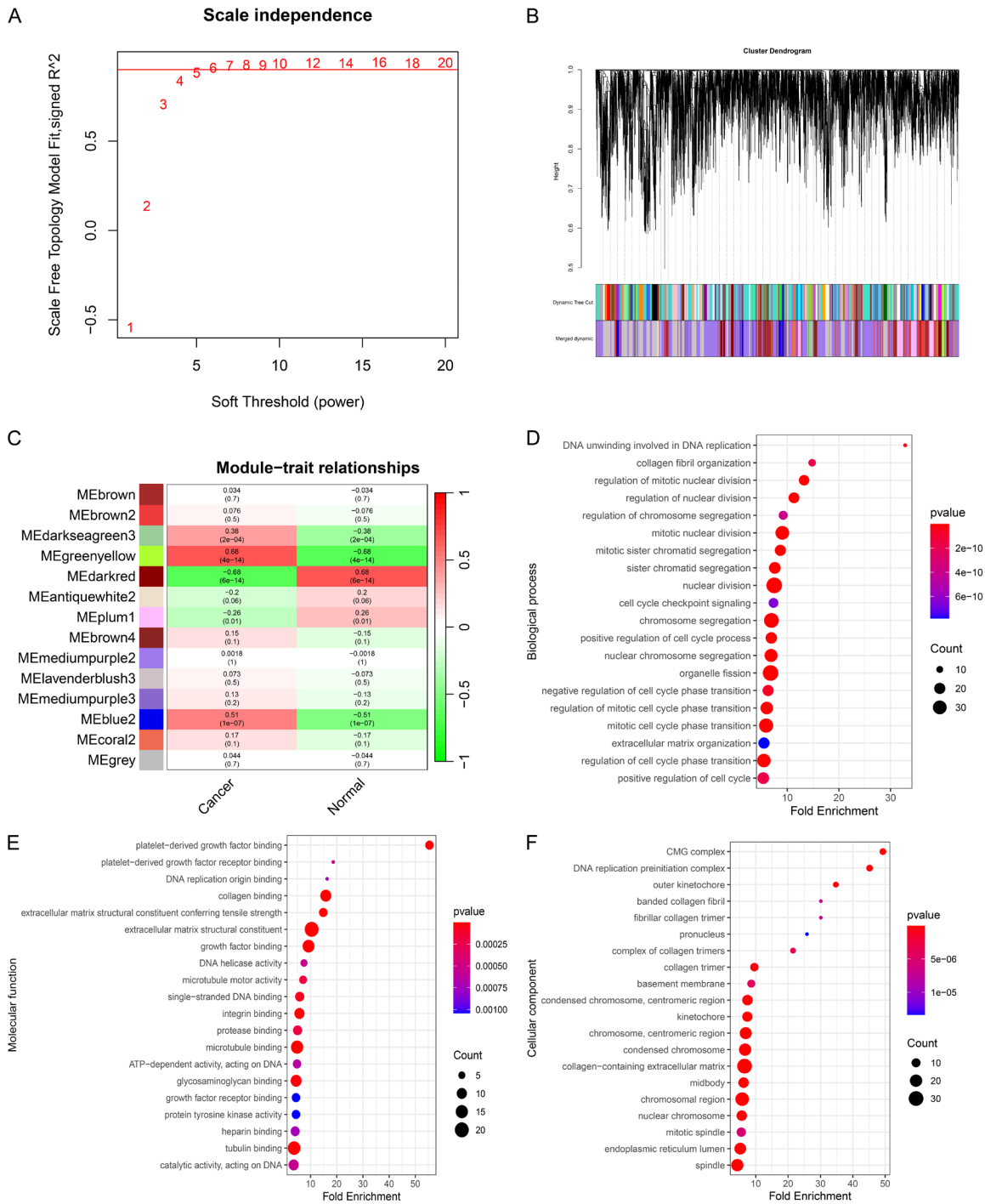
Figure 6. Identification of the functions of GC-related modules based on WGCNA and GO analysis. (A) Screening for the soft threshold, scale-free topological fit index (R^2). (B) WGCNA clustering dendrogram and module assignment. (C) Heatmap of module-feature correlations. Red indicates a positive correlation, and green indicates a negative correlation. (D) GO biological process, (E) molecular function and (F) cellular component analyses of positive modules identified by WGCNA.

(**Figure 7C**). With the degree algorithm of plug-in CytoHubba, the top 10 hub genes were identified from the PPI network, including APP,

PTEN, FBXW7, STAG2, CDC42, PPP2R1A, BRD4, KDR, ACTR2 and RAB11A (**Figure 7D**). Among these 10 genes, only APP was found to

CircRNA-miRNA-mRNA interaction network affecting the GC progression

A
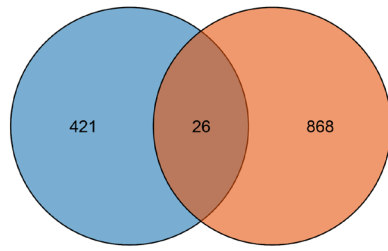
target genes of circRNA_0023685

genes in top 5 most enriched BPs

B
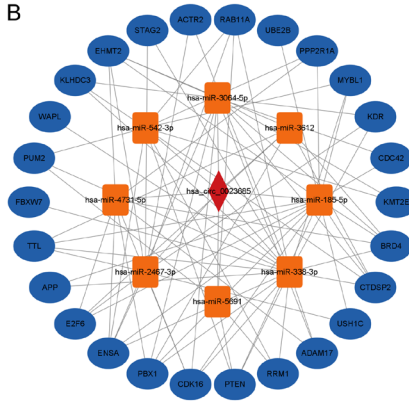
C
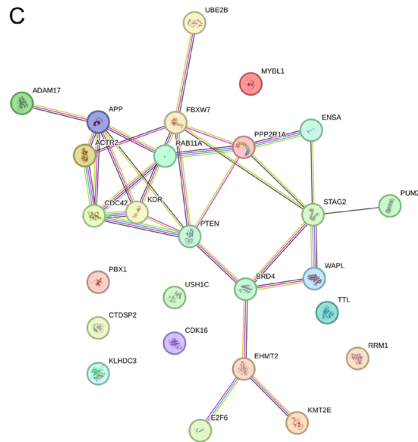
D
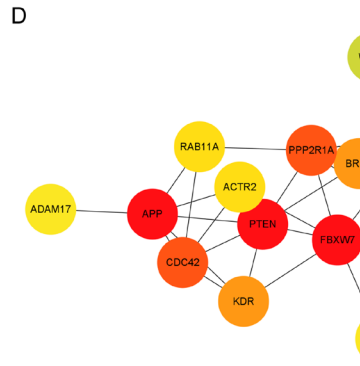
E **APP**
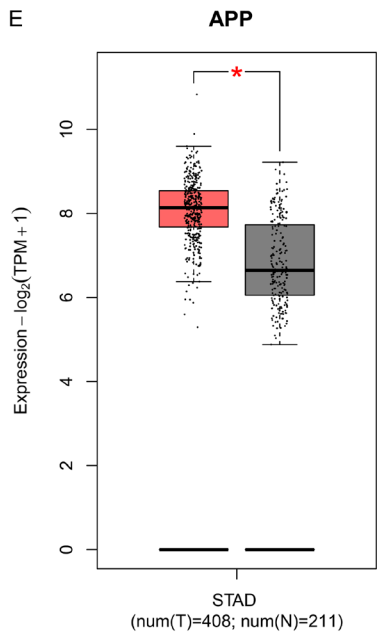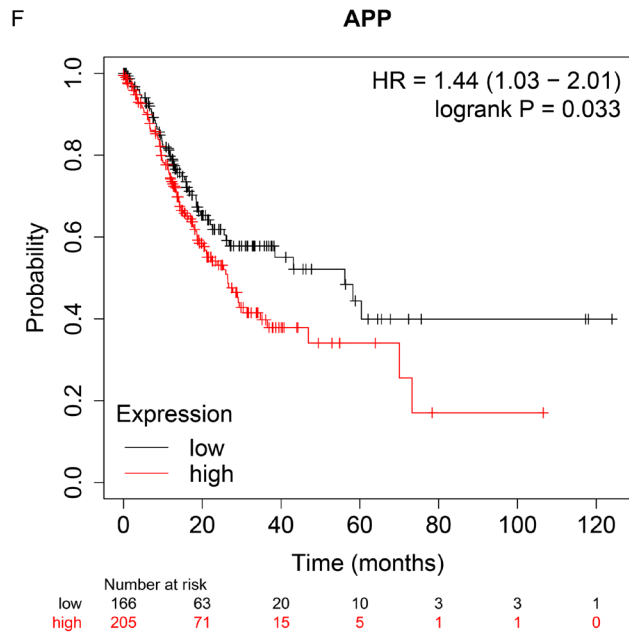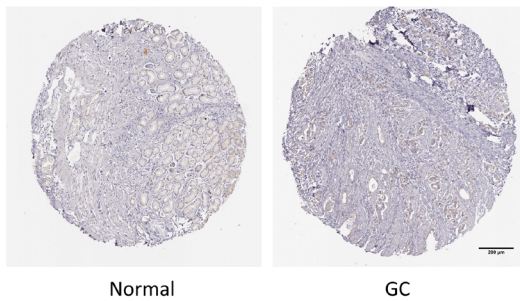
F **APP**

HR = 1.44 (1.03 − 2.01)
logrank P = 0.033

Expression
low
high

Time (months)

Number at risk

low	166	63	20	10	3	3	1
high	205	71	15	5	1	1	0

Expression − log₂(TPM + 1)

STAD
(num(T)=408; num(N)=211)

G

Normal   GC

Figure 7. APP was found to be a prognostic target through PPI network. A. Twenty-six genes overlapped between the genes in top 5 most enriched BPs and the predicted circRNA target genes. B. A regulatory circRNA-miRNA-mRNA network. C. A PPI network based on STRING database. D. Hub genes calculated by CytoHubba plug-in. E. APP is highly expressed in the stomach adenocarcinoma (STAD) dataset in TCGA. F. Kaplan-Meier (KM) curve showing the association of APP with overall survival (OS) in GC patients in the TCGA cohort. G. APP protein levels in normal stomach and GC were visualized by immunohistochemistry (IHC) in HPA. Bar = 200 μm. *; $P < 0.05$.

be highly expressed in GC and suggested a worse prognostic outcome, as determined through GEPIA and Kaplan-Meier plotter (**Figure 7E**, **7F**). The expression level of APP was validated by immunohistochemical assays from the HPA database, the result showed that it was expressed higher in tumor than in controls (**Figure 7G**).

Discussion

In this study, we discovered and verified circRNA_0023685 - a new circRNA that is substantially expressed in GC, as detected in both the plasma and tissues of patients. Furthermore, depletion of circRNA_0023685 was simultaneously verified by *in vitro* and *in vivo* experiments to inhibit the proliferation and invasion of GC cells. One typical mechanism by which circRNAs control gene expression is by binding to miRNAs and interfering with their ability to negatively regulate the expression of their target mRNAs. Through a series of bioinformatic analyses, a hub gene related to cell division process, APP, was finally identified as the candidate gene of circRNA_0023685 to promote GC.

In GC, one of the most malignant cancers, conventional therapies have limited clinical efficacy, and the median overall survival (mOS) time for advanced GC is only approximately 8 months [16]. Therefore, to increase the survival rate of GC, in addition to discovering new diagnostic biomarkers, it is crucial to find new therapeutic approaches. Differential expression of circRNAs has been observed in a variety of cancers, and targeting endogenous circRNAs has been investigated as a prospective therapeutic approach [17]. In addition, exogenous circRNAs could also be manufactured into medicinal products or vaccines with further research [18, 19]. It has been demonstrated that a synthesized circRNA can act as a miR-21 sponge to inhibit the proliferation of GC cells [20]. mRNA vaccines have received tremendous attention and emerged as the savior in the COVID-19 pandemic [21]. However,

mRNAs, which are usually in a linear form, are easily degraded, whereas circRNAs allow RNA retention for a longer period of time because of their covalently closed loop structure. This advantage reveals the therapeutic potential of circRNA vaccines. Additionally, circRNAs' ability to regulate gene expression has attracted much attention in cancer biology [22]. Because circRNAs are not easily degraded but are readily available, recent research has increasingly focused on their use as diagnostic biomarkers for cancer [13]. Tang *et al.* found that GC tissue-derived circ-KIAA1244 could be used as a novel circulating biomarker for the detection of GC [23]. Li *et al.* demonstrated that hsa_circ_002059 may be a potential novel stable biomarker for the diagnosis of GC by using patient tissues and plasma [24]. Future large-scale multicenter studies are clearly needed to validate the diagnostic and prognostic value of circRNA_0023685 in GC.

Amyloid precursor protein (APP) is a type I transmembrane protein which is highly conserved across species. Several studies have reported that different products produced during APP processing, in particular soluble APPα (sAPPα) and amyloid precursor protein intracellular domain (AICD), may play an important role in carcinogenesis [25, 26]. APP and its products can play an important role in cancer procession by participating in cell survival, cell adhesion, differentiation and migration [27-29]. Lim *et al.* found that APP cleavage products can have an oncogenic effect by affecting the cell cycle in breast cancer [30]. Moreover, circRNA_0023685 knockdown-mediated effect on GC cell progression was found, hinting that circRNA_0023685 could result in overexpression of APP through a circRNA-miRNA-mRNA network and thus promote GC. Further studies on the mechanism of APP to affect GC will be carried out.

In conclusion, we discovered a new circRNA, circRNA_0023685, that can promote GC by acting as a miRNA sponge and activating a

cascade of effects on APP. CircRNA_0023685 and APP may be useful as diagnostic markers and therapeutic targets for GC, a possibility that offers fresh perspectives on the detection and management of this disease. However, further research must be done to determine the precise mechanisms by which circRNAs influence the growth of GC.

Acknowledgements

Disclosure of conflict of interest

None.

Address correspondence to: Dr. Qi-Jun Wang, Faculty of Medical Laboratory Science, Ruijin Hospital, Shanghai Jiao Tong University School of Medicine, 197 Ruijin 2nd Road, Shanghai 200025, China. Tel: +86-21-54610176; E-mail: qijun_wang@sjtu.edu.cn; Dr. Yun-Wei Sun, Department of Gastroenterology, Ruijin Hospital, Shanghai Jiao Tong University School of Medicine, 197 Ruijin 2nd Road, Shanghai 200025, China. Tel: +86-21-64370045 Ext. 665242; E-mail: sun_yunwei@126.com

References

[1] Ma S, Zhou M, Xu Y, Gu X, Zou M, Abudushalamu G, Yao Y, Fan X and Wu G. Clinical application and detection techniques of liquid biopsy in gastric cancer. Mol Cancer 2023; 22: 7.

[2] Sung H, Ferlay J, Siegel RL, Laversanne M, Soerjomataram I, Jemal A and Bray F. Global cancer statistics 2020: GLOBOCAN estimates of incidence and mortality worldwide for 36 cancers in 185 countries. CA Cancer J Clin 2021; 71: 209-249.

[3] Tsai MM, Wang CS, Tsai CY, Huang HW, Chi HC, Lin YH, Lu PH and Lin KH. Potential diagnostic, prognostic and therapeutic targets of microRNAs in human gastric cancer. Int J Mol Sci 2016; 17: 945.

[4] Necula L, Matei L, Dragu D, Neagu AI, Mambet C, Nedeianu S, Bleotu C, Diaconu CC and Chivu-Economescu M. Recent advances in gastric cancer early diagnosis. World J Gastroenterol 2019; 25: 2029-2044.

[5] Chen CY, Hsu JS, Wu DC, Kang WY, Hsieh JS, Jaw TS, Wu MT and Liu GC. Gastric cancer: preoperative local staging with 3D multi-detector row CT--correlation with surgical and histopathologic results. Radiology 2007; 242: 472-482.

[6] Verduci L, Tarcitano E, Strano S, Yarden Y and Blandino G. CircRNAs: role in human diseases and potential use as biomarkers. Cell Death Dis 2021; 12: 468.

[7] Chen L and Shan G. CircRNA in cancer: fundamental mechanism and clinical potential. Cancer Lett 2021; 505: 49-57.

[8] Jeck WR and Sharpless NE. Detecting and characterizing circular RNAs. Nat Biotechnol 2014; 32: 453-461.

[9] Kristensen LS, Jakobsen T, Hager H and Kjems J. The emerging roles of circRNAs in cancer and oncology. Nat Rev Clin Oncol 2022; 19: 188-206.

[10] Wang J, Zhao X, Wang Y, Ren F, Sun D, Yan Y, Kong X, Bu J, Liu M and Xu S. circRNA-002178 act as a ceRNA to promote PDL1/PD1 expression in lung adenocarcinoma. Cell Death Dis 2020; 11: 32.

[11] Ge L, Sun Y, Shi Y, Liu G, Teng F, Geng Z, Chen X, Xu H, Xu J and Jia X. Plasma circRNA microarray profiling identifies novel circRNA biomarkers for the diagnosis of ovarian cancer. J Ovarian Res 2022; 15: 58.

[12] Wang S, Su W, Zhong C, Yang T, Chen W, Chen G, Liu Z, Wu K, Zhong W, Li B, Mao X and Lu J. An eight-circRNA assessment model for predicting biochemical recurrence in prostate cancer. Front Cell Dev Biol 2020; 8: 599494.

[13] Zou Y, Zheng S, Deng X, Yang A, Kong Y, Kohansal M, Hu X and Xie X. Diagnostic and prognostic value of circular RNA CDR1as/ciRS-7 for solid tumours: a systematic review and meta-analysis. J Cell Mol Med 2020; 24: 9507-9517.

[14] Wei L, Sun J, Zhang N, Zheng Y, Wang X, Lv L, Liu J, Xu Y, Shen Y and Yang M. Noncoding RNAs in gastric cancer: implications for drug resistance. Mol Cancer 2020; 19: 62.

[15] Li R, Jiang J, Shi H, Qian H, Zhang X and Xu W. CircRNA: a rising star in gastric cancer. Cell Mol Life Sci 2020; 77: 1661-1680.

[16] Li K, Zhang A, Li X, Zhang H and Zhao L. Advances in clinical immunotherapy for gastric cancer. Biochim Biophys Acta Rev Cancer 2021; 1876: 188615.

[17] He AT, Liu J, Li F and Yang BB. Targeting circular RNAs as a therapeutic approach: current strategies and challenges. Signal Transduct Target Ther 2021; 6: 185.

[18] Liu X, Zhang Y, Zhou S, Dain L, Mei L and Zhu G. Circular RNA: an emerging frontier in RNA therapeutic targets, RNA therapeutics, and mRNA vaccines. J Control Release 2022; 348: 84-94.

[19] Qu L, Yi Z, Shen Y, Lin L, Chen F, Xu Y, Wu Z, Tang H, Zhang X, Tian F, Wang C, Xiao X, Dong

X, Guo L, Lu S, Yang C, Tang C, Yang Y, Yu W, Wang J, Zhou Y, Huang Q, Yisimayi A, Liu S, Huang W, Cao Y, Wang Y, Zhou Z, Peng X, Wang J, Xie XS and Wei W. Circular RNA vaccines against SARS-CoV-2 and emerging variants. Cell 2022; 185: 1728-1744, e1716.

[20] Liu X, Abraham JM, Cheng Y, Wang Z, Wang Z, Zhang G, Ashktorab H, Smoot DT, Cole RN, Boronina TN, DeVine LR, Talbot CC Jr, Liu Z and Meltzer SJ. Synthetic circular RNA functions as a miR-21 sponge to suppress gastric carcinoma cell proliferation. Mol Ther Nucleic Acids 2018; 13: 312-321.

[21] Regev-Yochay G, Gonen T, Gilboa M, Mandelboim M, Indenbaum V, Amit S, Meltzer L, Asraf K, Cohen C, Fluss R, Biber A, Nemet I, Kliker L, Joseph G, Doolman R, Mendelson E, Freedman LS, Harats D, Kreiss Y and Lustig Y. Efficacy of a fourth dose of Covid-19 mRNA vaccine against omicron. N Engl J Med 2022; 386: 1377-1380.

[22] Kristensen LS, Hansen TB, Venø MT and Kjems J. Circular RNAs in cancer: opportunities and challenges in the field. Oncogene 2018; 37: 555-565.

[23] Tang W, Fu K, Sun H, Rong D, Wang H and Cao H. CircRNA microarray profiling identifies a novel circulating biomarker for detection of gastric cancer. Mol Cancer 2018; 17: 137.

[24] Li P, Chen S, Chen H, Mo X, Li T, Shao Y, Xiao B and Guo J. Using circular RNA as a novel type of biomarker in the screening of gastric cancer. Clin Chim Acta 2015; 444: 132-136.

[25] Arvidsson Y, Andersson E, Bergström A, Andersson MK, Altiparmak G, Illerskog AC, Ahlman H, Lamazhapova D and Nilsson O. Amyloid precursor-like protein 1 is differentially upregulated in neuroendocrine tumours of the gastrointestinal tract. Endocr Relat Cancer 2008; 15: 569-581.

[26] Al Khashali H, Ray R, Coleman KL, Atali S, Haddad B, Wareham J, Guthrie J, Heyl D and Evans HG. Regulation of the soluble amyloid precursor protein α (sAPPα) levels by acetylcholinesterase and brain-derived neurotrophic factor in lung cancer cell media. Int J Mol Sci 2022; 23: 10746.

[27] Hansel DE, Rahman A, Wehner S, Herzog V, Yeo CJ and Maitra A. Increased expression and processing of the Alzheimer amyloid precursor protein in pancreatic cancer may influence cellular proliferation. Cancer Res 2003; 63: 7032-7037.

[28] Sobol A, Galluzzo P, Weber MJ, Alani S and Bocchetta M. Depletion of amyloid precursor protein (APP) causes G0 arrest in non-small cell lung cancer (NSCLC) cells. J Cell Physiol 2015; 230: 1332-1341.

[29] Tsang JYS, Lee MA, Chan TH, Li J, Ni YB, Shao Y, Chan SK, Cheungc SY, Lau KF and Tse GMK. Proteolytic cleavage of amyloid precursor protein by ADAM10 mediates proliferation and migration in breast cancer. EBioMedicine 2018; 38: 89-99.

[30] Lim S, Yoo BK, Kim HS, Gilmore HL, Lee Y, Lee HP, Kim SJ, Letterio J and Lee HG. Amyloid-β precursor protein promotes cell proliferation and motility of advanced breast cancer. BMC Cancer 2014; 14: 928.
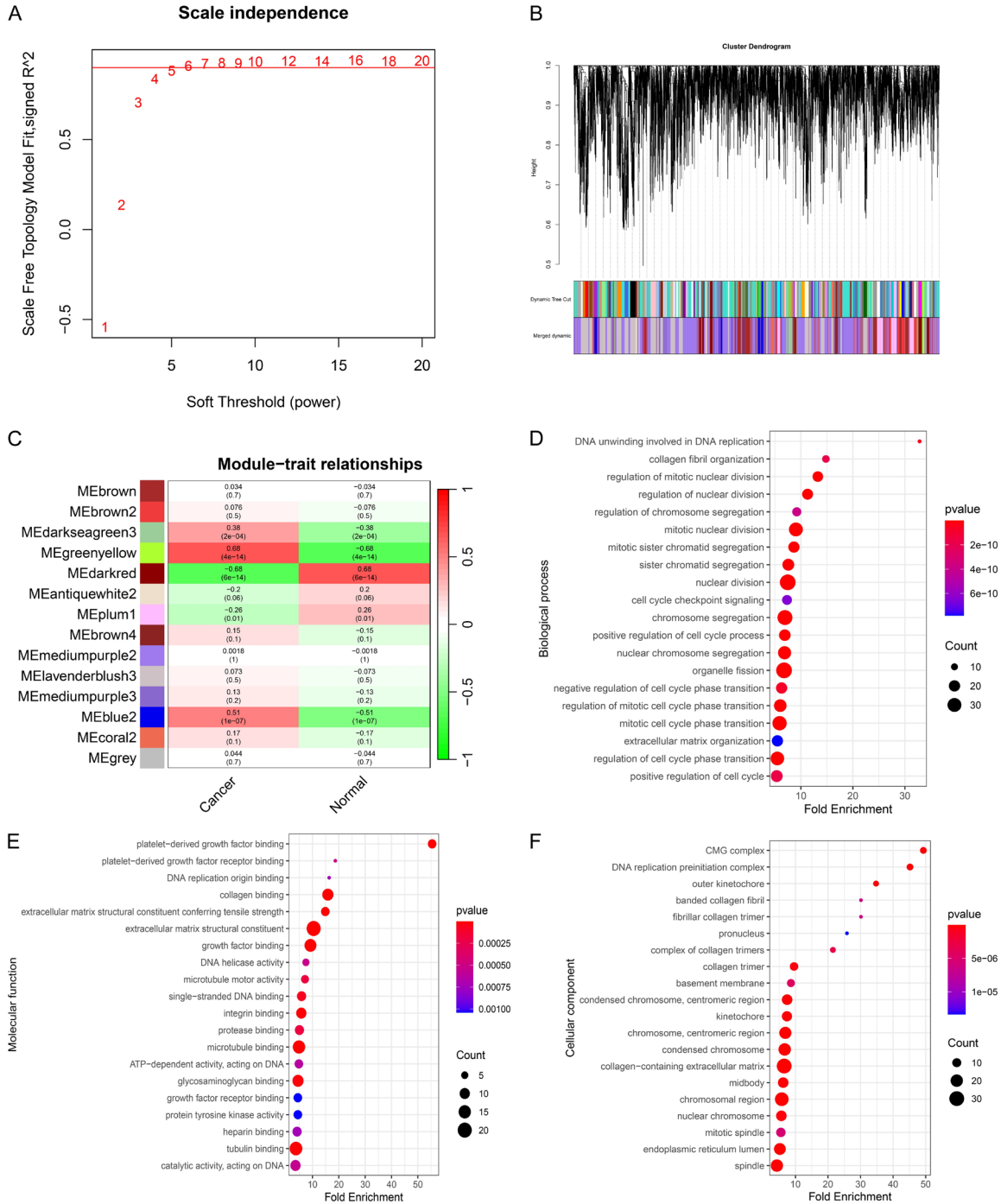
Supplementary Figure 1. Immune-related pathways play the main role in GC development in GSE113255, based on WGCNA and GO analysis. (A) Screening for the soft threshold, scale-free topological fit index (R^2). (B) WGCNA clustering dendrogram and module assignment. (C) Heatmap of module-feature correlations. Red indicates a positive correlation, and green indicates a negative correlation. (D) GO biological process, (E) molecular function and (F) cellular component analyses of positive modules identified by WGCNA.